

## Nulling Interferometry: Working on the Dark Fringe

E. Serabyn, J. K. Wallace, H. T. Nguyen, E. G. H. Schmidtlin and G. J. Hardy

*Jet Propulsion Laboratory, 4800 Oak Grove Drive, MS 171-113  
California Institute of Technology, Pasadena, CA 91109, USA*

### Abstract.

Deep nulling of both laser and thermal radiation has been demonstrated in the laboratory at visible wavelengths, by means of a rotational shearing interferometer (RSI) coupled to single-mode input and output fibers. To date, the best null depth obtained with a laser-diode source is  $8 \times 10^{-6}$ . The laser-diode null has also been passively stabilized to the  $\text{few} \times 10^{-5}$  level, implying a short-term interferometer stability of  $\approx 1$  nm. A transient null depth of  $2 \times 10^{-4}$  has also been achieved on a filtered, single-polarization, white-light source of 5% bandwidth. This null depth exceeds that which simple destructive interference in a standard “constructive” interferometer can provide, thus demonstrating the more achromatic nature of the central null in RSIs.

The interferometric cancellation, or “nulling”, of the incident light from nearby stars has the potential to enable the direct detection of their attendant planets and exozodiacal dust disks (Shao & Colavita 1992, Traub, Carleton & Angel 1996, Baudoz, Gay & Rabbia 1998, Hinz *et al.* 1998, Woolf & Angel 1998, Beichman, Woolf & Lindensmith 1999). However, to achieve adequate levels of starlight nulling, a very high degree of optical symmetry is required. Even with perfect optics, the intensities, polarizations and phases of the combining beams must all be matched to  $2\sqrt{N}$  (Serabyn 1999, in prep.), where the null depth,  $N$ , is defined as the ratio of the power throughputs at the interferometer’s destructive minimum and constructive maximum settings:

$$N = \frac{I_{\min}}{I_{\max}}. \quad (1)$$

Two fundamental limits must be overcome to enable deep nulling (in addition to practical matters such as symmetry and stability requirements). First, in normal Michelson interferometers (i.e., with constructive white-light fringes), dispersion limits the depth of the off-center interference minima to

$$\frac{I_{\min}}{I_{\max}} = \frac{1}{2} \left( 1 - \text{sinc} \left( \frac{\pi \Delta\lambda}{\lambda} \right) \right). \quad (2)$$

For bandwidths in the range 5 to 50 %, the destructive interference minima are limited to the range 0.05% to 5%, respectively. Deeper destructive interference thus calls for a more achromatic approach. One such approach is a relative field flip between the combining beams, such as is provided by a rotational shearing

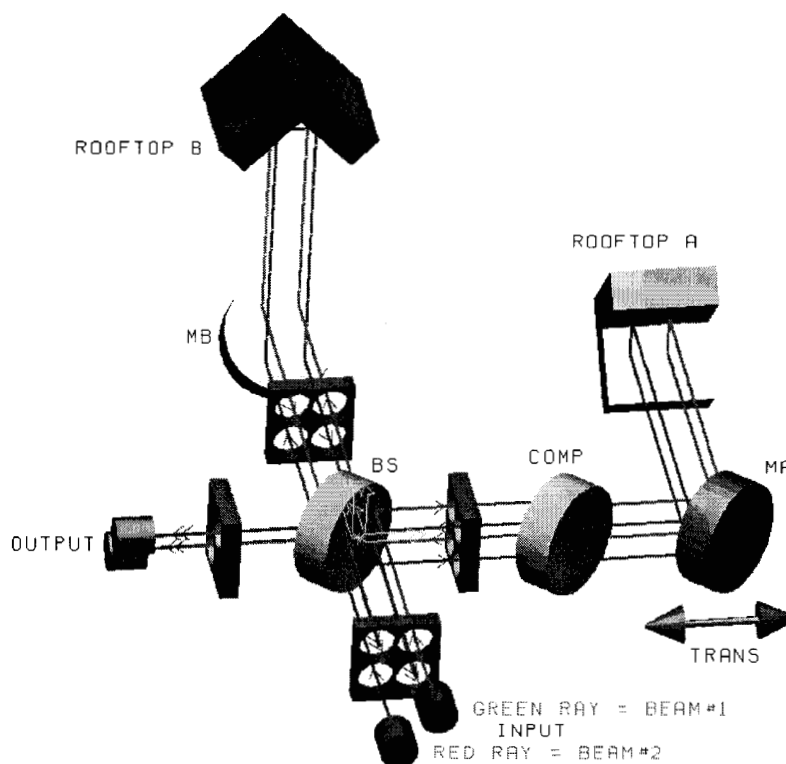


Figure 1. Nulling interferometer layout. Two input beams are sheared onto each other with reversed electric field vectors by the action of the two hollow rooftop mirrors shown. BS refers to the beamsplitter, COMP to the compensator, and MA and MB to two flat mirrors included to balance the number of s and p reflections in the RSI's arms. MA is mounted on a piezoelectrically-driven translation stage which provides a means of changing the OPD between the RSI's arms. The four aperture masks are aids to guide the eye; only the last one (which defines the common beam aperture) is actually present.

interferometer (RSI) of  $180^\circ$  shear (Diner *et al.* 1989, Shao 1991). Second, in the presence of wavefront imperfections, the null depth is limited to  $\approx 1 - S$ , where  $S$  is the Strehl ratio. It has been proposed that this limit, on the order of a few percent for typical optics, can be overcome by filtering the output point-spread function with a single-mode spatial filter (Shao 1991). In principle, an RSI coupled to a single-mode output fiber should thus provide a central achromatic null fringe of arbitrary depth.

As a prelude to planned interferometers with nulling capabilities such as the Keck Interferometer, the Space Interferometer Mission, and the Terrestrial Planet Finder (TPF), we have developed a testbed optical nulling interferometer at JPL over the course of the last year. Because of its significant advantages, the approach taken was a polarization-compensated orthogonal-rooftop RSI (Shao 1991), as shown in Figure 1. The advantages of such a beam combiner include a reliance solely on flat mirrors, near-perfect symmetry with respect to the two po-

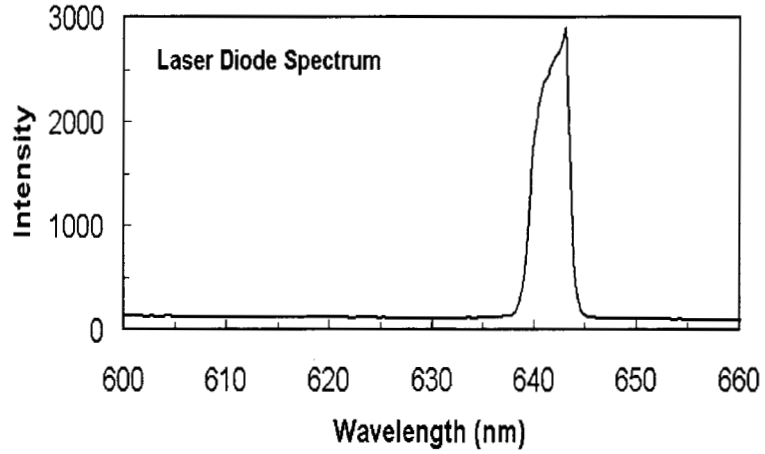


Figure 2. Low resolution (1 nm) spectrum of the Wave Optics laser diode used in our experiments. A higher resolution spectrum would show a series of narrow spikes attributable to individual laser modes.

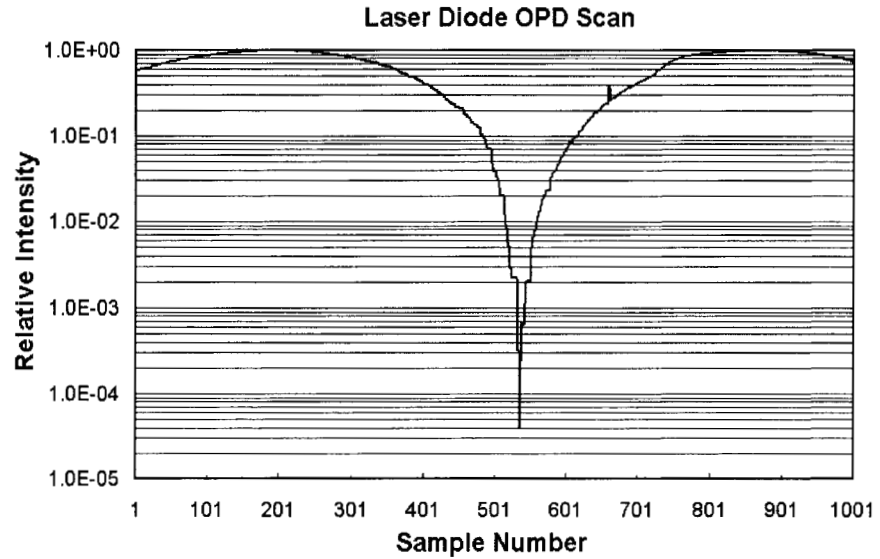


Figure 3. Nulling interferometer output power for a linear scan of the interferometer's OPD. The data were acquired on Dec. 30, 1998. The scan extends from one constructive fringe to the next, crossing through the zero OPD position near the center. At 50 Hz sampling, the total scan interval shown is 20 sec. The light source was the laser diode of Fig. 2, and the detector a Newport Corp. fiber-coupled detector. At zero OPD,  $N = 4 \times 10^{-5}$ .

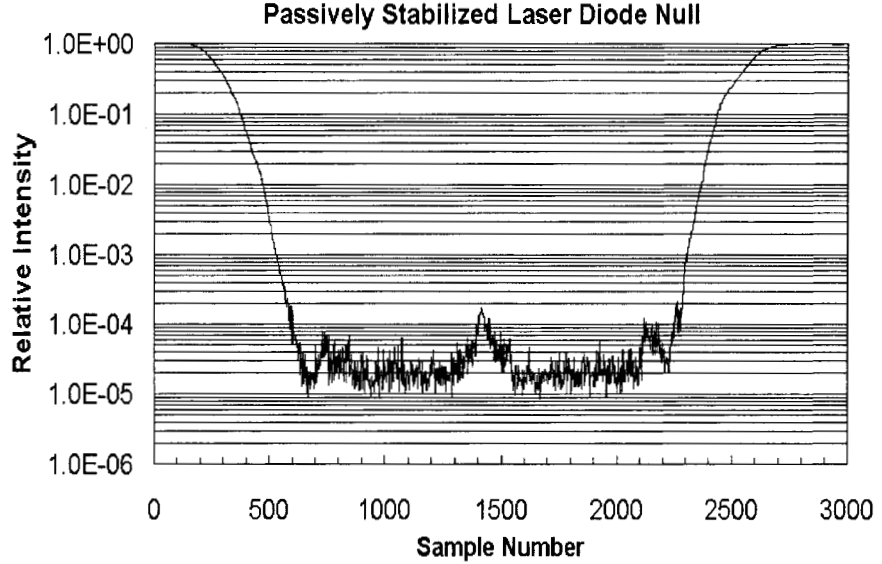


Figure 4. Null depth vs. time (at 50 Hz sampling) for manual tuning of the interferometer OPD. Beginning at an adjacent constructive interference peak, the interferometer OPD was manually zeroed (samples 0 to 850) with the PZT. For samples from  $\approx 850$  to 1350, the OPD was left free to drift. Thereafter, the OPD was manually re-zeroed, and then set free from  $\approx$  sample 1550 to 2100. Finally, the interferometer was manually retuned to the constructive peak. For the two  $\approx 10$  sec “free-OPD” intervals described,  $N$  is consistently  $< 6.2 \times 10^{-5}$ , and  $N_{\text{average}} \approx 2 \times 10^{-5}$ . The deepest transient null seen here is  $8.4 \times 10^{-6}$ .

larizations, and insensitivity to the beamsplitter’s exact reflection/transmission ratio (because the beamsplitter is used in double-pass). The optics are discussed briefly in Fig. 1. Here we focus on a summary of the current status of our experimental efforts.

Our initial experiments were conducted with a narrowband ( $\approx 0.5\%$  FWHM) laser-diode source (Fig. 2). Figures 3 and 4 show recent results obtained with this source. A scan of the nulling interferometer’s optical path difference (OPD) through the zero-OPD position shows a deep central null of  $4 \times 10^{-5}$  (Fig. 3). After making a number of improvements to the stability of our laboratory environment, the passive performance was improved to the point that we are now able to obtain short-term ( $\approx 10$  sec) stable nulls with average depths of  $2 \times 10^{-5}$ . The best transient nulls seen are typically 8 to  $9 \times 10^{-6}$  (Fig. 4), and these can be ascribed to fluctuations in the null (transmitted power) as the OPD fluctuates through zero (the noise level is well below these levels). Thus, a passive short-term interferometer stability of about 1 nm has been achieved.

Work has also begun on broader bandwidth nulls. Of course, our 0.5% BW laser diode is already significantly non-monochromatic, as evidenced by the fact that precise rotation of the compensator was necessary for deep nulls. Beyond this, we have also begun experiments with a bandpass-filtered thermal

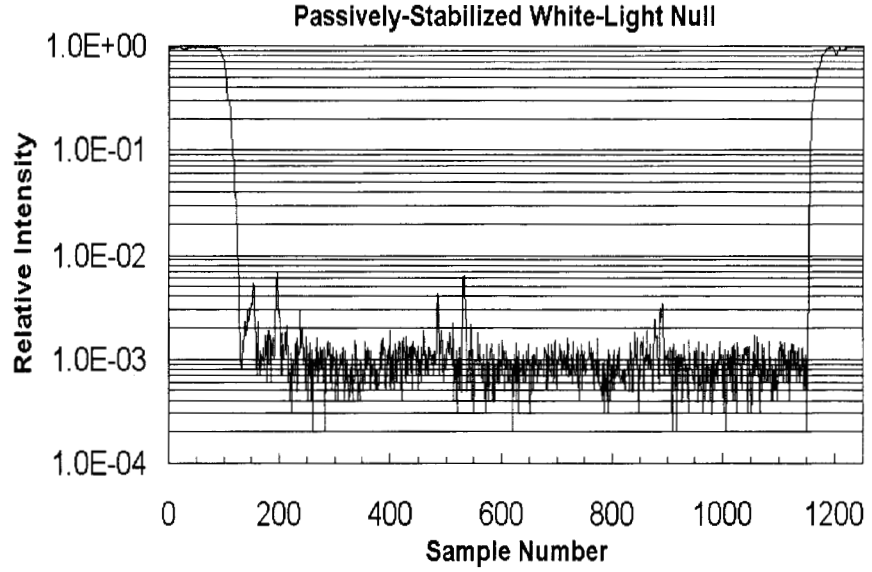


Figure 5. Null depth vs. time for manual tuning of the interferometer OPD as in Fig. 4, but for a filtered white-light source (5% BW, 1 polarization). Starting at the adjacent constructive interference peak, the OPD was again manually tuned to the null position, largely left free to drift between samples 200 and 1150, and then retuned to the constructive peak. For the greater part of the central 2 min (7 Hz sampling),  $N_{\text{average}} \approx 0.7 - 1.0 \times 10^{-3}$  (depending on the interval selected). The deepest transient null seen here (7 occurrences) is  $2 \times 10^{-4}$ .

white-light source (a fiber-coupled miniature light-bulb). After passage of the beam through parallel linear polarizers in the interferometer input and output beams, and filtering with a 5% bandwidth red filter, null depths as deep as  $N = 2 \times 10^{-4}$  have been seen while passively stabilized near null (Fig. 5). According to Eqn. 2 (which is plotted in Fig. 6), this null level is significantly better than destructive interference in a standard Michelson, or “constructive white light”, interferometer can provide ( $5 \times 10^{-4}$  for a 5% bandwidth). Surpassing this limit thus establishes the achromatic nature of the central null, and at the same time suggests the potential for even deeper and broader nulls.

A summary of our current status is provided in Figure 6, in the form of a plot of the best null depths obtained to date (actually the highest rejection ratio, or  $N^{-1}$ ) vs. radiation bandwidth. The data points in Fig. 6 were not obtained with a common instrumental tuning, so this plot should not be considered as an instantaneous performance curve. On the other hand, several things are evident in the plot. First, the very deep nulls obtained confirm the viability of the fiber-coupled RSI approach for the generation of deep nulls: in particular, both the achromatic nature of the field cancellation, and the efficacy of wavefront correction via single-mode spatial filtering are verified. Second, our best laser nulls are already only one order of magnitude short of the null depths considered necessary for the viability of the TPF mission. Finally, the main remaining

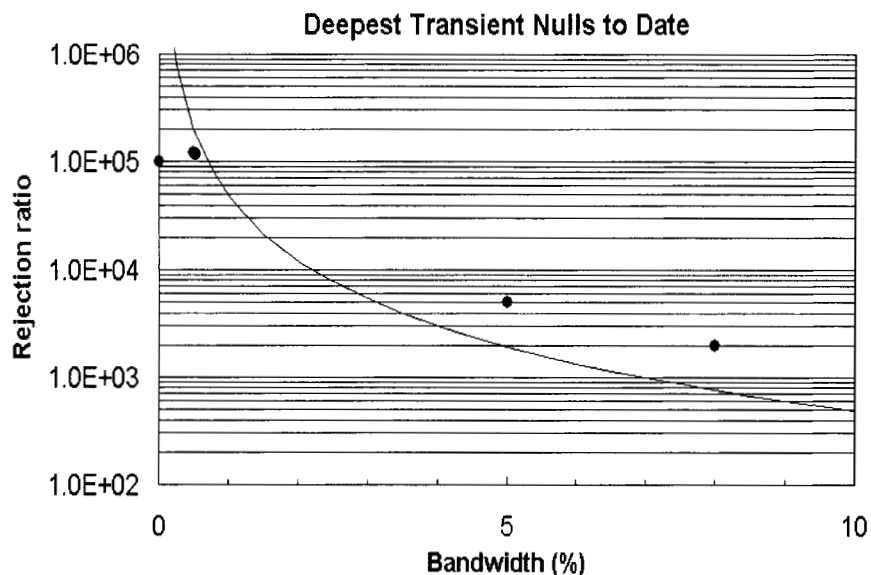


Figure 6. Deepest nulls obtained to date vs. radiation bandwidth. The point at zero bandwidth refers to a HeNe laser, that at 0.5% BW to our laser diode, and those at 5% and 8% BW to filtered, fiber-coupled, single-polarization white-light. The plotted curve gives the maximum rejection possible with a standard Michelson interferometer (Eqn. 2).

uncertainty is the nulling bandwidth attainable, and so our next experimental goal is clearly the demonstration of a broadband null.

**Acknowledgments.** We thank M. Shao for helpful discussions, and R. G. Dekany and M. Colavita for graciously providing laboratory space. This research was carried out at JPL, under contract with NASA.

## References

- Baudoz, P., Gay, J. & Rabbia, Y. 1998, in *Brown Dwarfs and Extrasolar Planets*, ed. R. Rebolo, E.L. Martin & M. Osorio, ASP Conf. Ser. Vol. 134, 254
- Beichman, C.A., Woolf, N.J. & Lindensmith, C.A. 1999, *Terrestrial Planet Finder*, JPL publ. 99-3
- Diner, D.J. 1989, in *The Next Generation Space Telescope*, ed. P.Y. Bely, C.J. Burrows & G.D. Illingworth, 133
- Hinz, P.M. *et al.* 1998, *Nature* 395, 251
- Shao, M. 1991, in *Space Astronomical Telescopes and Instrumentation*, ed. P.Y. Bely & J.B. Breckinridge, Proc. SPIE, 1491, 347
- Shao, M. & Colavita, M.M. 1992, *ARA&A* 30, 457
- Traub, W.A., Carleton, N.P., & Angel, J.R.P. 1996, in *Science with the VLT Interferometer*, ed. F. Paresce, 80
- Woolf, N. & Angel, J.R.P. 1998, *ARA&A* 36, 507